Anti-Vibration Control of Turntable Ladders by a Steel Rope-Hydraulic Control System

Van Tinh Nguyen
Faculty of Mechanical Engineering, Hanoi University of Civil Engineering, Vietnam
tinhnv@huce.edu.vn
(corresponding author)

Received: 31 December 2022 | Revised: 1 February 2023 | Accepted: 9 February 2023

ABSTRACT

Anti-vibration control of turntable ladders is effective by controlling the steel ropes inserted in the hollow handrails. Previous studies that considered idealized conditions, such as ignoring friction, piston mass, and hydraulic oil compressibility, can not be strongly generalized. This study addresses these problems by describing in detail the equipment serving the anti-vibration solution, building a mathematical model for the steel rope hydraulic control system considering the above factors, and controlling the rapid extinguishing of vibrations on a model simulated in Matlab-Simulink. Furthermore, the simulation of the relationship between the control signal and oil flow through the proportional distribution valve produced a signal flow curve that was asymptotic to the actual. The results showed a difference compared to previous studies. Although the solution was only implemented on the lowest ladder section with the most unfavorable conditions, the time for vibration on the top ladder reached amplitudes of 3 and 5mm in 3 and 5s for empty and full baskets, respectively.

Keywords-aerial extension ladder; anti-vibration control; dynamic equation; steel rope hydraulic control; turntable ladder

I. INTRODUCTION

The study on vibration reduction, fast vibration quenching, and anti-swing for load transport equipment has high scientific and practical significance. Various control methods have been proposed to bring the load to the desired position quickly and accurately [1-4]. This activity makes more sense for turntable ladders because they transport rescued people and should help them feel safe in a rescue basket. Authors in [5-7] presented effective control methods to eliminate vibrations on turntable ladders. In [8-11], a new solution was presented to eliminate vibrations and overcome large static displacements on ladders, putting steel ropes inside the hollow of the handrails. These steel ropes were tensioned and controlled by small hydraulic cylinders mounted on the handrail tops, using the available hydraulic power of the truck. This method showed that the tension of the steel ropes had a positive effect on the anti-vibration on the top ladder [8] and the control of the steel ropes rapidly reduced the vibrations on the ladder [9]. In [10], stress reduction on key ladder elements and significant reduction of static displacements were demonstrated by evaluating the ladder structure with additional steel ropes according to the standards [12-13]. The hydraulic circuit design and cylinder control according to the control principle [9] were presented in [11]. However, the control system model in [11] was not very accurate and comprehensive, as it did not consider the elasticity of hydraulic oil, ignored friction forces and the mass of the piston rod, and used approximate mathematical models for the flow-signal curve. This study investigated the detailed structure of the anti-vibration device, the dynamic model of the steel rope hydraulic control system, the establishment of a mathematical model of the system with an accurate flow-signal curve, and the practice of controls for rapid suppression of vibrations on turntable ladders.

II. STEEL ROPE-HYDRAULIC CONTROL SYSTEM

Figure 1 shows the structure of the devices attached to the hollow handrails of a ladder, omitting the ladder structure. The hydraulic cylinder is integrated with the position sensor mounted on the lower end of the handrail.

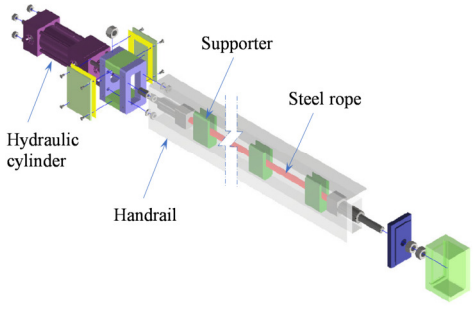

Fig. 1. Added components into a hollow handrail.

A threaded joint connects the piston rod to one end of the steel rope. The steel rope with a high damping coefficient is threaded in the handrail and supported by supports. The

supports are lightweight plastic evenly spaced to eliminate the rope sag. The other end of the rope is fixed by a threaded joint to the other end of the ladder. Additional devices were implemented in the lowest ladder section for anti-vibration to match the size of the 30m set including the three ladder sections described in [14]. The control on the third ladder is the most effective [9]. The most effective vibration control is when placing the actuator closest to the fixed end of a cantilever beam [15]. Figure 2 shows the mechanical model of the ladder structure, the steel rope, and the force generated by the cylinder. The control system commands the actuator to generate a force to reduce vibration. This force moves with a variable velocity rule that follows or nearly follows a predefined rule. Based on the data in [8-11], all parameters in this model were entirely determined.

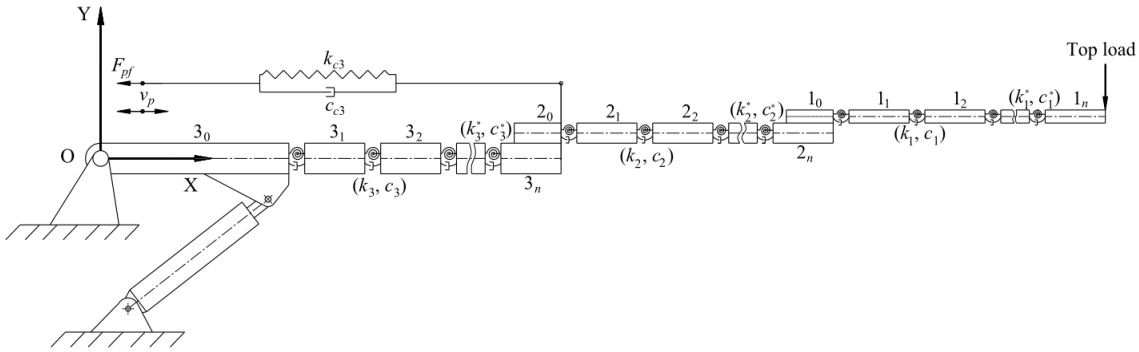

Fig. 2. Multi-body dynamics model of ladder set and steel rope in hollow handrails.

Figure 3 shows the model of the steel rope hydraulic control system. During the operation of the proportional directional valve, when the P-A ports are connected, the high-pressure hydraulic oil pushes the piston to the left to pull the steel rope. In contrast, when the A-T ports are connected, the oil in the cylinder chamber flows to the tank through the pressure sequence valve due to the tension of the rope pulling the piston. In this model, k_{c3} and c_{c3} are the stiffness and damping coefficients of the ropes in the third ladder section, A_p, p_p are the area and the pressure of the oil chamber, and x_p and x_r are the displacements of the piston and the remaining fixed end of the steel rope, respectively.

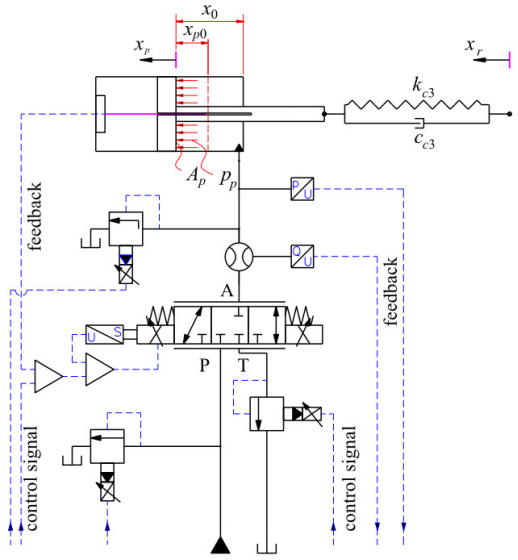

Fig. 3. Mechanical model of steel rope-hydraulic control system.

III. EQUATION OF MOVEMENT

According to [9], during the vibration control performance, the acceleration vector of the addition motion is determined as:

$$\ddot{\eta} = -M(t)^{-1}C(t)\dot{\eta} - M(t)^{-1}K(t)\eta + M(t)^{-1}(F + k_{FD}k_{contr}D) \quad (1)$$

where $\ddot{\eta}$, $\dot{\eta}$, and η are the acceleration, velocity, and displacement vectors of the addition motion of the rigid bodies, $M(t)$, $C(t)$, and $K(t)$ are the mass matrix, the damping matrix, and the stiffness matrix, D is the load matrix including T_i (bending moment) and D_i (damping load) caused by the steel rope in the i-th ladder section, F is the load matrix excluding the load components caused by the steel rope, and $k_{FD} = \partial F(t)/\partial D$ with $F(t)$ being the total generalized load matrix.

$$k_{contr} = diag[1 \quad 1 \quad 1 \quad 1 \quad k_{T3} \quad k_{D3}] \quad (2)$$

where k_{T3} and k_{T3} are the controlling factors corresponding to T_3 and D_3 in the third ladder section, respectively. The motion equation of the piston is given by:

$$p_pA_p - k_{c3}\Delta l_{ca3} - c_{c3}\Delta \dot{l}_{ca3} - F_f = m_p\ddot{x}_p \quad (3)$$

where Δl_{ca3}, $\Delta \dot{l}_{ca3}$ represent the length change range and the length change speed of the steel rope, F_f is the friction force, m_p is the piston mass, and $\ddot{x}_p$ is the piston acceleration. The exact determination of the friction force is very complicated and it is necessary to conduct experiments on each specific object. To simplify the simulation, it was determined as follows [16]:

$$F_f = \begin{cases} F_s + c_p \cdot |p_pA_p| & \text{for } \dot{x}_p > v_0 \\ (F_s + c_p \cdot |p_pA_p|)\frac{\dot{x}_p}{\dot{x}_0} & \text{for } -\dot{x}_0 \le \dot{x}_p \le v_0 \\ -F_s - c_p \cdot |p_pA_p| & \text{for } \dot{x}_p < -v_0 \end{cases} \quad (4)$$

where v_0 is the velocity whose value is a very small positive around zero, F_s=$10^5 A_p$, and c_p=2%. The change range of the steel rope length during work is given by:

$$\Delta l_{ca3} = x_p + x_{p0} - x_r \quad (5)$$

and the length change speed of the steel rope is given by:

$$\Delta \dot{l}_{ca3} = \dot{x}_p - \dot{x}_r \quad (6)$$

with x_r being the longitudinal displacement of the upper end of the handrail. The dynamic equation for the oil compressibility inside the cylinder chamber can be written as [17]:

$$\dot{p}_p = \frac{\beta_o}{V_c}\left(Q_x - \dot{V}_c\right) \quad (7)$$

where $\dot{p}_p$ denotes the change rate of the chamber pressure, β_o is the oil bulk modulus, V_c denotes the oil volume, and Q_x denotes the rate of flow entering the chamber.

$$V_c = V_{oc} + A_p\left(x_p + x_0\right) \quad (8)$$

$$\dot{V}_c = A_p \dot{x}_p \quad (9)$$

where x_0 is the oil length in the cylinder chamber when it is set to create the initial tension load, x_p is the displacement of the piston, and V_{OC} is the oil volume in the pipe.

Replacing (8) and (9) in (7) gives:

$$\dot{p}_p = \frac{\beta_o}{(V_{oc}+A_p x_0)+A_p x_p}\left(Q_x - A_p \dot{x}_p\right) \quad (10)$$

The flow rate depends on the pressure drop which is the pressure difference between the inlet and outlet ports and the corresponding nominal flow. This is detailed in:

$$Q_x = Q^*_{Nom} \cdot \sqrt{\frac{\Delta p_x}{\Delta p_{Nom}}} \quad (11)$$

where Δp_{Nom} is the pressure drop when the flow rate is nominal, and the command signal is maximum, Δp_{Nom}=5×10^5Pa, Δp_x is the pressure drop when working, and Q^*_{Nom} is the flow rate depending on the command signal. Q^*_{Nom} is determined as:

$$Q^*_{Nom}/Q_{Nom} = f(u) \quad (12)$$

where u=U/U_{max}, U is the control voltage, U_{max} is the maximum control voltage, and Q_{Nom} is the nominal flow at U_{max}.

Equation (10) is rewritten in the case of the piston pulling the steel rope:

$$\dot{p}_p = \frac{\beta_o\left(f(u)\cdot Q_{Nom}\cdot\sqrt{\frac{p_{oh}-p_p}{\Delta p_{Nom}}}-A_p\dot{x}_p\right)}{(V_{oc}+A_p x_0)+A_p x_p} \quad (13)$$

and in the case of the steel rope pulling the piston:

$$\dot{p}_p = \frac{\beta_o\left(f(u)\cdot Q_{Nom}\cdot\sqrt{\frac{p_p-p_{ou}}{\Delta p_{Nom}}}-A_p\dot{x}_p\right)}{(V_{oc}+A_p x_0)+A_p x_p} \quad (14)$$

with p_{oh} and p_{ou} being the pressure at P and T ports, respectively.

IV. ANTI-VIBRATION CONTROL

Based on the parameters and the original characteristic curve of the proportional directional valve presented in [18], to simplify the numerical simulation process in its half corresponding to the positive signal, (12) can be approximated as:

$$\frac{Q^*_{Nom}}{Q_{Nom}} = \begin{cases} 0 & \text{for } 0 \le u < \frac{1}{10} \\ \frac{327u^2}{100} - \frac{63u}{100} + \frac{3}{100} & \text{for } \frac{1}{10} \le u \le \frac{25}{100} \\ \frac{37u}{30} - \frac{7}{30} & \text{for } \frac{25}{100} < u \le 1 \end{cases} \quad (15)$$

Figure 4 shows the original flow curve and the approximate curve generated by (15). They almost coincide.

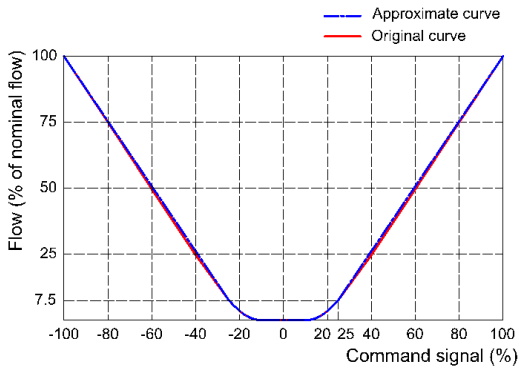

Fig. 4. Flow characteristic according to command signal percentage.

The steel rope hydraulic control system model was established in Matlab-Simulink, as shown in Figure 5. The main parts of this model are:

- Ladder structure model: a subsystem created from the ladder dynamic model in Matlab-Simulink, as presented in [9].
- Signal generator: The velocity sensor at the top of the third ladder section provides a signal to the control signal generator, which is the original signal that is smoothed and amplified before reaching the valve. As the original signal is taken from the ladder structure model, the phase delay of the control signal must be considered. Here, the tensioner model starts 30ms after the ladder model. A delay time of 4ms was selected. When the amplitude of the vibration at the top ladder is small enough, the signal generator will stop working. This amplitude value can be preset.
- Function blocks of the hydraulic devices: They determine the dynamic parameters of the piston and the oil pressure in the chamber through (3) and (13)-(15).
- Damping load block: It receives the piston and rope end velocity signals and creates the damping force ($c_{c3}\Delta\dot{l}_{ca3}$).
- Rope tension block: It has the function of generating rope tension ($k_{c3}\Delta l_{ca3}$) based on the longitudinal deformation of the steel rope.

Table I shows the modeling parameters. The largest vertical vibration at the top ladder may occur when the ladder is horizontal and fully extended. Therefore, this study implements anti-vibration control in this ladder state.

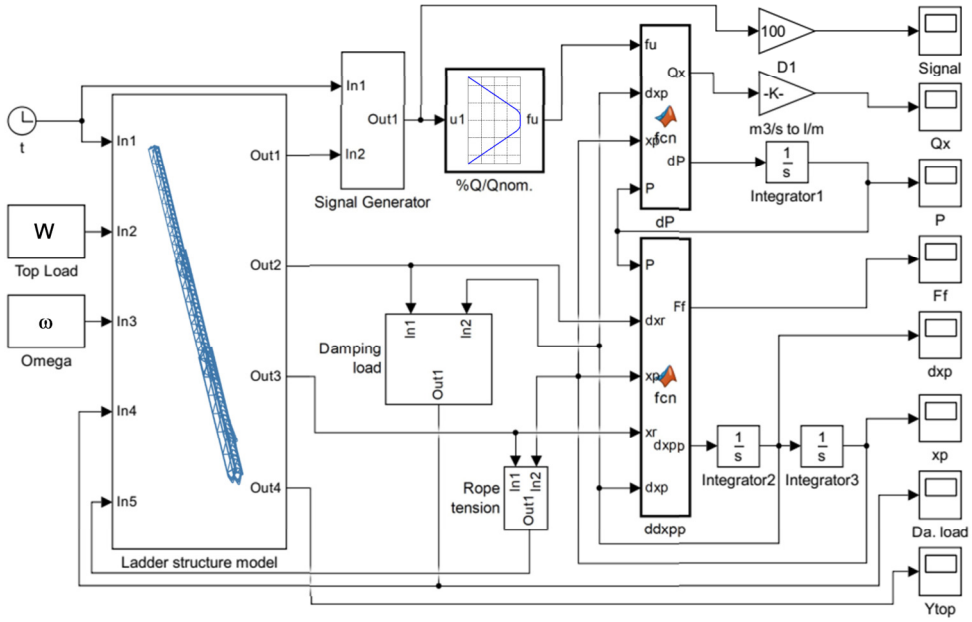

Fig. 5. Steel rope-hydraulic control system model in Matlab-Simulink.

TABLE I. MODEL PARAMETERS OF CONTROL SYSTEM

β_o (Pa)	x_0 (m)	x_{p0} (m)	m_p (kg)	A_p (m^2)
1.8×10^9	0.02	0.01	1.1	10^{-3}
V_{oc} (m^3)	p_{oh} (Pa)	p_{ou} (Pa)	c_{c3} (Ns/m)	k_{c3} (N/m)
2.1×10^{-4}	21×10^6	5×10^6	1650	1.29×10^6

Figures 6-12 show the parameters obtained during the control process, including control signal, oil flow, oil pressure, friction force, piston speed and displacement, and damping force in the empty basket case. Figure 13 shows the displacement graphs on the top ladder for both basket cases. Despite the control signal's late start and phase delay, the vibration control through the steel rope hydraulic control system was highly effective. Compared to [9] and [11], these results overcome the expected effect after control. In the empty basket case, the vibration amplitude after only 3s of control reaches 3mm for the top ladder instead of 67mm. The control systems in the other studies need more than 8s to achieve this amplitude. In case of a full basket, the vibration amplitude of the top ladder after 5s of control reaches 5mm compared to the others that need more than 14s to achieve such amplitude.

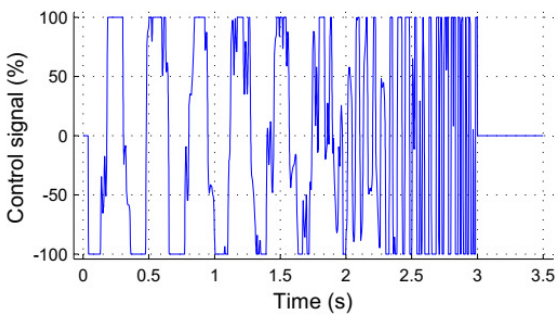

Fig. 6. Control signal percentage.

In addition to the steel rope having the effect of damping, the hydraulic equipment also suppresses the vibration when operating. The pressure and flow rate values for the cylinders presented in Figures 7-8 are suitable for the hydraulic system of a turntable ladder. The speed and displacement of the piston shown in Figures 10-11 are also consistent with the kinematic parameters of a piston used to control a precise motion system.

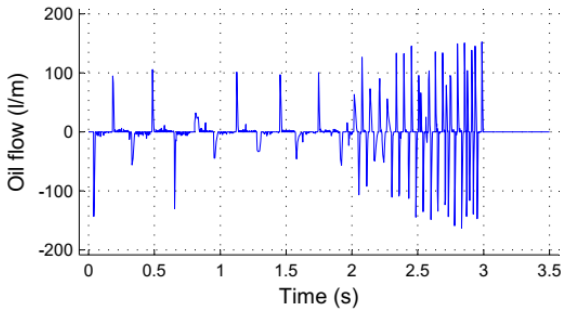

Fig. 7. Oil flow through a proportional directional valve.

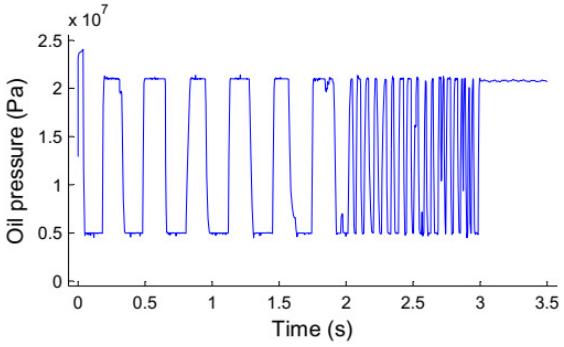

Fig. 8. Oil pressure in the cylinder chamber.

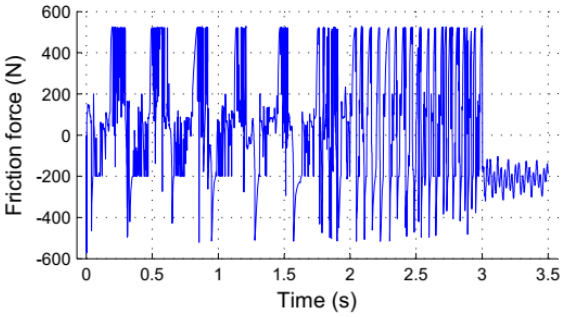

Fig. 9. Friction force between piston and cylinder.

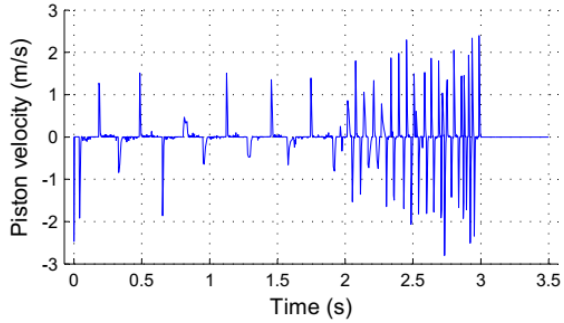

Fig. 10. Piston velocity.

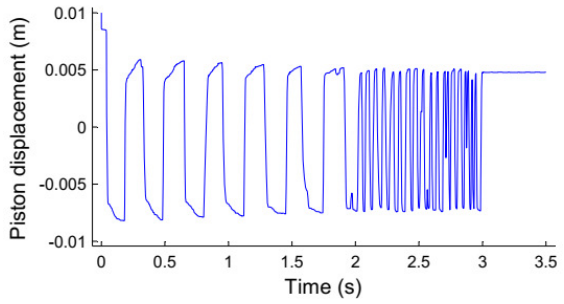

Fig. 11. Piston displacement.

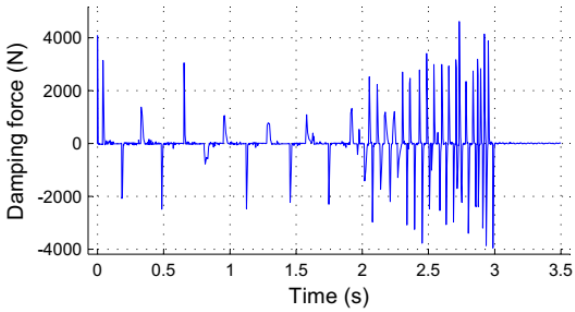

Fig. 12. Damping force.

V. CONCLUSION

The paper presented a new approach to anti-vibration methods for turntable ladders. It also shows the feasibility of carrying out the novel control solution presented in [9] with available devices in the market. A steel rope hydraulic system dynamic model, including tension and damping load of steel the ropes, friction force between the piston and the cylinder, oil compressibility, piston mass, and the proportional directional valve characteristics, was established and simulated. This model was combined with the ladder set's multi-body dynamics model to control the vibration's rapid quenching at the top ladder with a unique signal generator. Friction, oil compressibility, and the inertia force of the piston significantly influence the damping of the ladder's vibrations. This model extinguished vibrations by controlling the steel rope hydraulic system more efficiently, controlling only the steel ropes. The vibration reduction rate was approximately three times faster than in other studies.

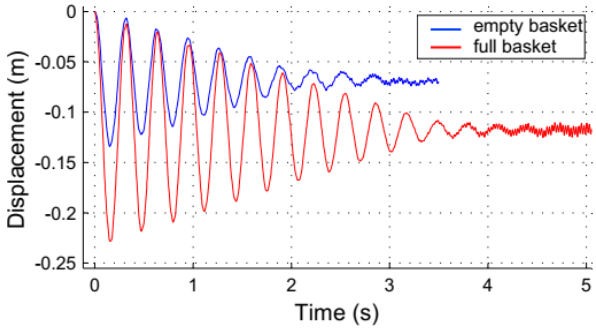

Fig. 13. Displacement of the top ladder.

REFERENCES

[1] J. Neupert, E. Arnold, K. Schneider, and O. Sawodny, "Tracking and anti-sway control for boom cranes," *Control Engineering Practice*, vol. 18, no. 1, pp. 31–44, Jan. 2010, https://doi.org/10.1016/j.conengprac.2009.08.003.

[2] B. Spruogis, A. Jakstas, V. Gican, V. Turla, and V. Moksin, "Further Research on an Anti-Swing Control System for Overhead Cranes," *Engineering, Technology & Applied Science Research*, vol. 8, no. 1, pp. 2598–2603, Feb. 2018, https://doi.org/10.48084/etasr.1774.

[3] L. A. Tuan and L. V. Duong, "Neural fractional-order control of telescopic truck cranes," *Applied Mathematical Modelling*, vol. 108, pp. 807–824, Aug. 2022, https://doi.org/10.1016/j.apm.2022.04.006.

[4] M. D. Duong, Q. T. Dao, and T. H. Do, "Settling Time Optimization of a Critically Damped System with Input Shaping for Vibration Suppression Control," *Engineering, Technology & Applied Science Research*, vol. 12, no. 5, pp. 9388–9394, Oct. 2022, https://doi.org/10.48084/etasr.5242.

[5] N. Zimmert, A. Kharitonov, and O. Sawodny, "A new Control Strategy for Trajectory Tracking of Fire–Rescue Turntable Ladders," *IFAC Proceedings Volumes*, vol. 41, no. 2, pp. 869–874, Jan. 2008, https://doi.org/10.3182/20080706-5-KR-1001.00149.

[6] N. Zimmert, A. Pertsch, and O. Sawodny, "2-DOF Control of a Fire-Rescue Turntable Ladder," *IEEE Transactions on Control Systems Technology*, vol. 20, no. 2, pp. 438–452, Mar. 2012, https://doi.org/10.1109/TCST.2011.2116021.

[7] A. Pertsch and O. Sawodny, "Modelling and control of coupled bending and torsional vibrations of an articulated aerial ladder," *Mechatronics*, vol. 33, pp. 34–48, Feb. 2016, https://doi.org/10.1016/j.mechatronics.2015.11.009.

[8] V. T. Nguyen, T. Schmidt, and T. Leonhardt, "Effect of pre-tensioned loads to vibration at the ladder tip in raising and lowering processes on a turntable ladder," *Journal of Mechanical Science and Technology*, vol. 33, no. 5, pp. 2003–2010, May 2019, https://doi.org/10.1007/s12206-019-0402-2.

[9] V. T. Nguyen, T. Schmidt, and T. Leonhardt, "A new active vibration control method on a ladder of turntable ladders," *Journal of Mechanical Science and Technology*, vol. 35, no. 6, pp. 2337–2345, Jun. 2021, https://doi.org/10.1007/s12206-021-0506-3.

[10] V. T. Nguyen, "Effect of pre-tensioned rope tensions on a ladder structure of turntable ladders," *Journal of Science and Technology in Civil Engineering (STCE) - HUCE*, vol. 16, no. 1, pp. 138–151, Jan. 2022, https://doi.org/10.31814/stce.huce(nuce)2022-16(1)-12.

[11] V. T. Nguyen, "A solution to increase the flexural stiffness and quickly extinguish vibrations on a ladder of turntable ladders," *Tạp chí Khoa học Công nghệ Xây dựng (KHCNXD) - ĐHXDHN*, vol. 16, no. 3V, pp. 138–149, Jul. 2022, https://doi.org/10.31814/stce.huce(nuce)2022-16(3V)-11.

[12] "Rules for the Design of Hoisting Appliances," Federeation Europeenne de la Manutention, FEM 1.001, Oct. 1998.

[13] "High rise aerial appliances for fire and rescue service use - Turntable ladders with combined movements - Safety and performance requirements and test methods," European Committee for Standardization, European Standard EN 14043:2014, 2014.

[14] M. J. Burman, S. E. Goodson, and J. D. Aiken, "Telescopic aerial ladders; components; and methods," US20090101436A1, Apr. 23, 2009.

[15] K. G. Aktas and I. Esen, "State-Space Modeling and Active Vibration Control of Smart Flexible Cantilever Beam with the Use of Finite Element Method," *Engineering, Technology & Applied Science Research*, vol. 10, no. 6, pp. 6549–6556, Dec. 2020, https://doi.org/10.48084/etasr.3949.

[16] M. K. Bak and M. R. Hansen, "Analysis of Offshore Knuckle Boom Crane - Part One: Modeling and Parameter Identification," *MIC Journal*, vol. 34, no. 4, pp. 157–174, Jan. 2013, https://doi.org/10.4173/mic.2013.4.1.

[17] M. G. Rabie, *Fluid Power Engineering*, 1st ed. New York, NY, USA: McGraw Hill, 2009.

[18] "Hydraulic Valves Industrial Standard," Parker Hannifin Corporation, 2015.